

# A Multiobjective Damping Function for Coordinated Control of Power System Stabilizer and Power Oscillation Damping

Jose D. Herrera, Mario A. Rios

**Abstract**—This paper deals with the coordinated tuning of the Power System Stabilizer (PSS) controller and Power Oscillation Damping (POD) Controller of Flexible AC Transmission System (FACTS) in a multi-machine power systems. The coordinated tuning is based on the critical eigenvalues of the power system and a model reduction technique where the Hankel Singular Value method is applied. Through the linearized system model and the parameter-constrained nonlinear optimization algorithm, it can compute the parameters of both controllers. Moreover, the parameters are optimized simultaneously obtaining the gains of both controllers. Then, the nonlinear simulation to observe the time response of the controller is performed.

**Keywords**—Balanced realization, controllability Grammian, electromechanical oscillations, FACTS, Hankel singular values, observability Grammian, POD, PSS.

## I. INTRODUCTION

THE stability of the power system is one of the most important aspects in the operation and security of electrical systems, as it refers to the ability of the system to reach a steady state after a disturbance [1].

Once electric power systems are developed in an interconnected form in which spontaneous oscillations at low frequencies in the order of 0.1 to 3 Hz could be presented [2]. These oscillations are caused by faults, increases in charges, lost control, small changes in the reference voltage regulator automatic voltage (AVR), and so on. Such fluctuations tend to stay for a long time, and in some cases, tend to grow causing the separation of power systems if there is no adequate damping. Moreover, low frequency oscillations cause limitations on the ability to transfer power, preventing transmission lines operating at maximum capacity [1], [2].

Generally, some generators are provided with additional controls that are PSS which provide additional damping to oscillations of the generator rotor through auxiliary signs of stabilization. On the other hand, FACTS can be used to improve system stability by means of a supplementary control signal for POD [1], [2]. However, lack of coordination of local control in the PSS and POD could cause destabilizing interactions in the power system when both are present.

J. D. Herrera is with the Department of Electrical Engineering and Electronics, School of Engineering, Universidad de los Andes, Bogotá, Colombia (e-mail: hm.jose10@uniandes.edu.co).

M. A. Rios is with the Department of Electrical Engineering at Universidad de los Andes, Bogota, Colombia. (phone: +571-3394949 ext. 2826, e-mail: mrios@uniandes.edu.co).

Some researches propose a coordination between generators' PSS and FACTS' POD controller devices to improve the overall system performance. Some of these methods use nonlinear complex simulations; [3] and [4] propose hybrid fuzzy controllers, and [5] deals with an optimization problem by solving a sequential quadratic programming using the dual algorithm.

Other methods are based on the linearization model of electric power system. First, [6] uses projective controls, which is expressed as a linear quadratic regulator to obtain a full-state feedback control. Secondly, [7] is based on the concept of induced torque coefficients and it proposes an optimization linear programming whose objective function is to minimize the weighted sum of the stabilizer gains. The last one designs a decentralized multivariable excitation controllers using a linear quadratic regulator [8].

In contrast to these methods, the solution of this paper is a methodology to coordinate a PSS and POD gains based on an algorithm of optimization whose objective is to reach a damping index of critical eigenvalues of the power system by minimizing the fitness in which the mutual influence of both PSS and POD controller parameters is considered. The development of this method requires a dynamic model reduction order technique based on the product of the observability and controllability grammians using the formulation described in these paper [9]-[11].

This paper is organized as: Section II introduces the basic structure of the employed PSS and POD controllers. Section III presents the test system used. Section VI presents the results obtained from the optimized controller gains. Finally, Section V presents the conclusions.

## II. PSS AND POD CONTROLLER

This paper presents a methodology of coordinated tuning of gains when each controller, PSS and POD, are placed in generators and FACTS devices. Thus, the block diagram of typical PSS (Fig. 1) and POD (Fig. 2) is used.

The values of each parameter that comprises the typical structure are  $T_w$ ,  $T_1$ ,  $T_2$ ,  $T_3$ ,  $T_4$ .  $T_w$  is a time constant and can assume values between 3 to 20 s [1], [2], [12], [13]. This parameter is not critical, and its value depends on the function and the modes which will be damped [1], [2], [12], [13].  $T_1/T_2$  and  $T_3/T_4$  are time constants and must be fixed to provide damping on the frequency range where the oscillations are likely to occur [1], [2], [12], [13]. These parameters provide a phase compensation between the power system plant and the

PSS controller, and the number of the lead-lag block depends on the amount of phase compensation that requires the power system [1], [12]-[14]. The frequency range of interest is between 0.1 and 5 Hz, where electromechanical oscillations to damp are placed [12]-[14].

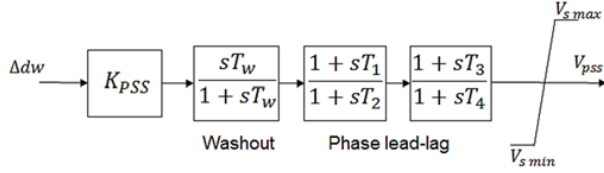


Fig. 1 Block diagram representation PSS [1]

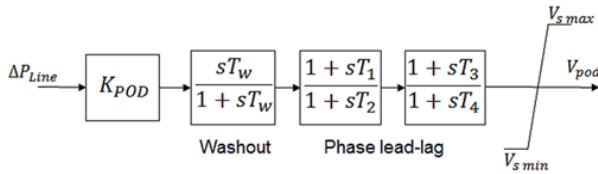


Fig. 2 Block diagram representation POD [1]

This paper computes the gains of PSS and POD controllers simultaneously using a genetic algorithm [15]-[17]. The primary procedure is as follows: *i*-Select the input signals for modal analysis, *ii*-Reduce the model order for suitable control design, *iii*-Compute the coordinated gains of PSS and POD using a genetic algorithm.

#### A. Selection of the PSS and POD Controller Input Signal

The aim is to reach the design coordinate of PSS and POD. The first step is the selection of generators and FACTS devices where the controllers will be located. The second step is to select the input signal to both controllers. Therefore, the linear full-order dynamic model of the system around a nominal operating point and, after obtaining the matrices of the system's state space model, the analysis modal is made through controllability and observability. The following properties are the main characteristics of a suitable input signal:

- 1) The input signal should be locally measurable.
- 2) The electromechanical modes to be damped should be observable in the input signal.
- 3) The input signal must yield correct control actions.
- 4) The input signal with best responses are associated with the frequency of the machine.

#### B. Model Reduction

The behavior of a dynamic system in low frequency electromechanical oscillations ranging from 0.1 to 3 Hz, is usually expressed as a set of nonlinear differential and algebraic (DAE) equations of the following form [1], [9], [12]:

$$\begin{aligned} \dot{x} &= f(x, z, u) \\ 0 &= g(x, z, u) \\ y &= h(x, z, u) \end{aligned} \quad (1)$$

where  $f$  and  $g$  are the vectors of differential and algebraic equations and  $h$  is a vector of output equations.

The nominal model system is linearized without the PSS and POD controllers; thus, the state space model is linearized around of a critical operating point and can be represented by [9], [10], [12]:

$$\begin{aligned} \dot{x} &= Ax + Bu \\ y &= Cx \end{aligned} \quad (2)$$

The order reduction technique is based on a computation algorithm of a subspace of the product of the controllability and observability grammians using the development propose in [10] that allows the retention of unstable modes in the reduced system.

The reduction method is applicable to multivariable systems (MIMO) with more than one input and one output signals. The advantage of developing low-order models suitable for control design applications is that the computational cost is reduced, and the optimization algorithms are faster.

The Hankel Singular Values (HSV) method was used as the order reduction method. It is also termed balanced truncation; this technique is split into: the most important states and the least important states with poor controllability and observability.

The least important states are established based on the values that the HSV brings. The singular value of the product of controllability and observability grammian is  $\sigma(\tilde{P}\tilde{Q}) = \text{diag}(\sigma_1, \sigma_2, \dots, \sigma_n)$ , thus  $\sigma$  are the HSV of the state space model system [9].

For stable systems, a balanced realization is an equivalent realization in which the controllability and observability grammians are equal and diagonal, and this diagonal forms the Hankel Singular Values ( $\sigma$ ). Small entries in  $\sigma$  indicate the states that can be removed to simplify the model.

The balanced realization in  $\tilde{x}$ , is obtained by a similarity transformation:

$$\begin{aligned} \tilde{A} &\triangleq P_1^{-1}AP_1 \\ \tilde{B} &\triangleq P_1^{-1}B \\ \tilde{C} &\triangleq CP_1 \end{aligned} \quad (3)$$

where  $P_1$  is the transformation matrix [10]. Under these conditions, it is revealed that the grammians of the model ( $A, B, C$ ) are similar and diagonal and they are computed by [9]:

$$\begin{aligned} \tilde{P} &= P_1^{-1}PP_1^{-T} \\ \tilde{Q} &= P_1^TQP_1 \end{aligned} \quad (4)$$

where  $P$  and  $Q$  are the solutions of the system of Lyapunov equations [12]:

$$\begin{aligned} PA^T + AP + BB^T &= 0 \\ QA + A^TQ + C^TC &= 0 \end{aligned} \quad (5)$$

In (5),  $A, B, C$  are the matrices from the continuous model in (2) linearized around the operating point. The matrix

transformation  $P_1$  which satisfies the balanced realization definition is termed as a contragredient transformation and is obtained by:

$$P_1 = L_p V \Sigma^{-1/2} \quad (6)$$

where  $L_p, V$ , and  $\Sigma^{-1/2}$  can be determined by using the Cholesky factors from  $P$  and  $Q$ , and the singular values decomposition [11].

When the balanced realization is finished, the next step is to truncate the new system. The truncation algorithm is based on the singular values of the matrix product  $\tilde{P}\tilde{Q}$ . The HSV are defined below:

$$\sigma_i = \lambda_i(\tilde{P}\tilde{Q})^{1/2} \quad (7)$$

The truncated model is then applied to obtain the reduced ignoring the least significant states of the system model [12]:

$$\begin{aligned} \dot{x} &= A_r x + B_r u \dot{x} = A_r x + B_r u \\ y &= C_r x \end{aligned} \quad (8)$$

After reducing the model, the frequency response of both models, the full order model and the reduced model, are compared in order to guarantee that at low frequency region the gain difference is small [12].

### C. Optimization Problem Formulation

The aim of the coordination tuning is to left-shift the electromechanical modes, while minimizing the damping ratio. The optimization problem is formulated in (9), the calculation is performed through the weighted sum of the objective functions:

$$\begin{aligned} \min J &= \alpha \cdot \xi_{interarea} + \beta \cdot \xi_{area1} + \gamma \cdot \xi_{area2} \\ \text{s.t.} \quad & A_r x + B_r = 0 \\ & K_{min} \leq K_{pss} \leq K_{max} \\ & K_{min} \leq K_{pod} \leq K_{max} \\ & \xi_i \geq 5\% \end{aligned} \quad (9)$$

where  $\alpha, \beta$  and  $\gamma$  correspond to the weights associated with each damping ratio  $\xi_i$ , respectively. The weights are multiples major or equal to the unit.

The constraints are the set of algebraic DAE equations in the operating point such that the damping of each mode will be greater than a specified value (which may be different for each mode) and the parameters of each controller as inequalities.

The mathematical formulation for damping ratio is expressed as:

$$\xi_i = \frac{-\sigma}{\sqrt{\sigma^2 + \omega^2}} \quad (10)$$

$\lambda_i = \sigma \pm j\omega$  represents the eigenvalues of the electromechanical modes that will be damped.

### D. Genetic Algorithm Optimization Technique

The optimization problem in (9) is a multi-objective problem and it can be posed as follows:

- 1) The minimization of a function that involves weighting the objective multiples (Damping of each one of electromechanical modes that are considered).
- 2) Vector function of multiple damping with weighting factors.

The pseudocode describing the genetic algorithm is as follows:

- 1) Generate an initial population.  $t = 0$ .
- 2) Evaluate the objective function (9), for each one of the individual.
- 3) Calculate fitness of each individual.
- 4) Apply the *Selection* operator over the  $N$ -individuals of the population.
- 5) Apply *Crossover* and *Mutation*; on the individuals selected previously.
- 6) Verify the stop criterion. If it is not satisfied, return to step 2, incrementing the iteration counter  $t = t + 1$ , else, finish the algorithm execution.

Fig. 3 shows the algorithm for the coordinated tuning based on genetic algorithms.

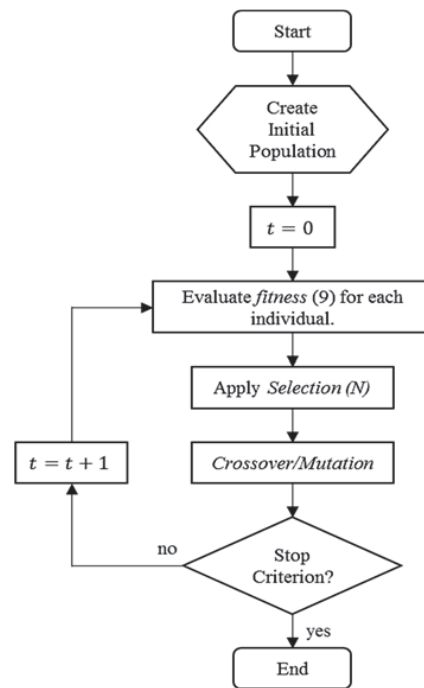


Fig. 3 Flow chart of the optimization coordinated tuning

The optimization problem formulation in this paper allows considering all the selected operating points. The multi-objective function calculates the best gains for each controller and also it adds damping to electromechanical modes.

Each feasible solution of the optimization problem is represented by a vector of real numbers  $x = [K_{pss}, K_{pod}]$ .

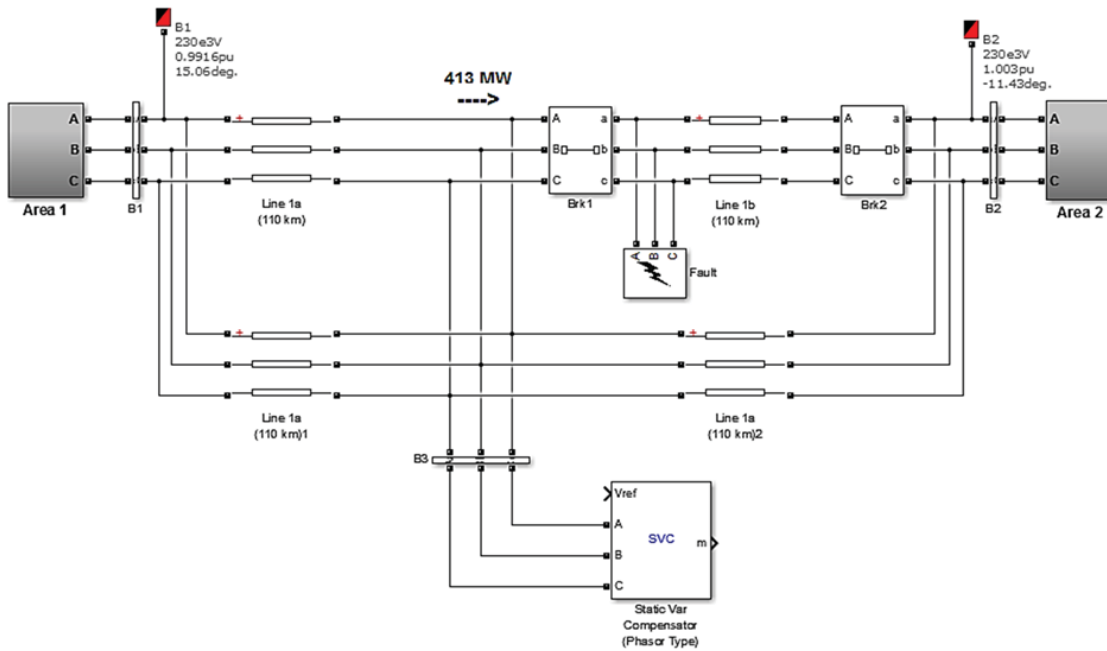


Fig. 4 Kundur's four-machine two-area modified with SVC [1], [18]

### III. KUNDUR'S FOUR MACHINE TWO-AREA TEST SYSTEM

Fig. 4 shows the test system that corresponds to the well-known Kundur's power system [1], [18], modelled at SimPower. The case of study is modified with a SVC device. In this system, all machines are equipped with static exciters and one PSS in the second machine located in the area 1, also one POD located in the SVC FACTS device. For the coordinated PSS and POD control scheme, the following considerations are taken into account:

- 1) The rotor speed deviation is selected as a PSS input signal and the local signal applied to the POD controller is the active power flow through the area 1 to area 2. The modal analysis is carried out to select the candidate signals by controllability and observability.
- 2) The test system is simulated for a disturbance which is a three-phase short circuit of four cycle duration in the middle of a line between area 1 and area 2.

Fig. 5 shows the active power flow throughout the area 1 to area 2 when a fault in the middle of the interconnection lines between area 1 and 2 occurs. As it is shown, the system presents undamped oscillations leading to instability.

The system dominant eigenvalues without any supplementary controller are given in Table I. From this, the system has two local modes and one inter-area mode with a damping ratio less than 5%. These modes are the critical electromechanical modes.

A modal analysis shows the three dominant modes in Table I, and the first one is an inter-area mode ( $\omega_n = 0.64$  Hz) involving the whole area 1 against area 2. The second one is a local mode of area 1 ( $\omega_n = 1.15$  Hz) involving this area's machine against each other, and the last one is a local model of area 2 ( $\omega_n = 1.12$  Hz) involving the other machines against

each other.

TABLE I  
EIGENVALUES OF TEST SYSTEM – BASE CASE

Eigenvalue	Frequency Hz	Damping Ratio
$0.1157 \pm 4.0633i$	0.6461	-0.0284
$-0.6564 \pm 7.2825i$	1.1590	0.0897
$-0.6822 \pm 7.0508i$	1.1221	0.0963

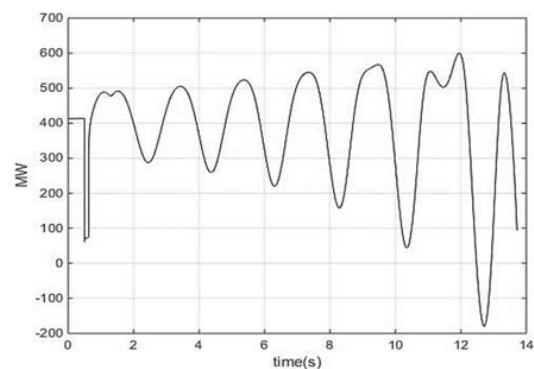


Fig. 5 Active power flow through interconnection of area 1 to area 2 - without supplementary control

The range of Bode Diagram shows the behavior of the reduced model in low frequency and it includes the local and inter-area modes. The errors in the reduced model are small, and the expected result is great for the design of the controllers.

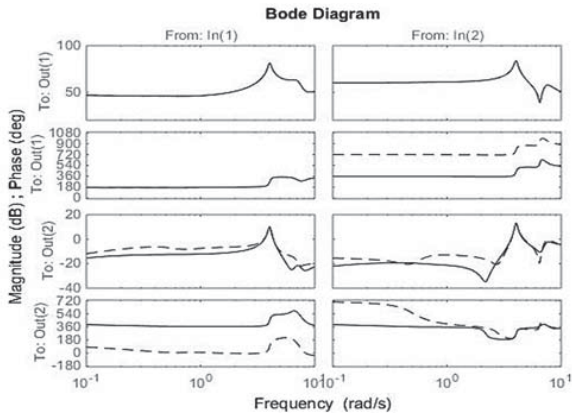


Fig. 6 Frequency of the original and the reduced 18<sup>th</sup> order system

A. Controller Parameters

Table II defines the boundary limits for PSS and POD gains, taken from the previous researches [1], [2], [19], [20]. The PSS and POD consist of three blocks; a phase compensation block, a signal washout and a gain.

Range	$T_w$	$T_1$	$T_2$
$1 \leq K \leq 200$	10s	0.06s	0.02s

The phase compensation should maximize the bandwidth within which lag phase should remain at less than 90°, because if it exceeds 90°, damping will decrease by increasing the gain [13]. The frequency at which the compensation phase reaches 90° is  $f_c = 1/2\pi\sqrt{T_1 T_2}$ , and the values of  $T_1$  and  $T_2$  could be calculated by  $f_c$ . Greater  $f_c$  means a greater bandwidth, but this result represents a reduction in the damping of the local modes, to achieve a better damping in the local modes  $f_c < 5$  Hz or to be around this value [13].

The washout block has the variable  $T_w$  and is chosen to give bandpass effect to the carrying signals that contain the local and inter-area modes [9]. For local modes,  $T_w = 1 - 2$  s is satisfactory [1], [14]. For inter-area modes,  $T_w = 10 - 20$  s is necessary [1], [14]. An improvement in the first swing stability is achieved  $T_w = 10$  s.

The gain  $K$  should be set at a value corresponding to the maximum damping  $\xi$ ; for this reason, this variable has an interval in which the algorithm will choose the best value.

Only the leading compensation block is taken account and its variables are assumed as shown in Table II. The optimization function has been applied to search for the optimal gains of the PSS and SVC POD controller.

B. Base Case with  $\xi \geq 5\%$

The optimization problem is performed for different damping ratios to observe the sensibility, and the weighting factors are  $\alpha = 50$ ,  $\beta = 25$ , and  $\gamma = 25$ . The damping ratio minor requires a greater weight.

Fig. 7 shows the Pole-Zero map for the case basis with a damping ratio higher than 5%.

Table III presents the gains of both controllers with a damping ratio higher than 5%.

	K	$T_w$	$T_1$	$T_2$	$\xi$
PSS	38.531	10.0s	0.06s	0.02s	0.05
POD	36.965	10.0s	0.06s	0.02s	

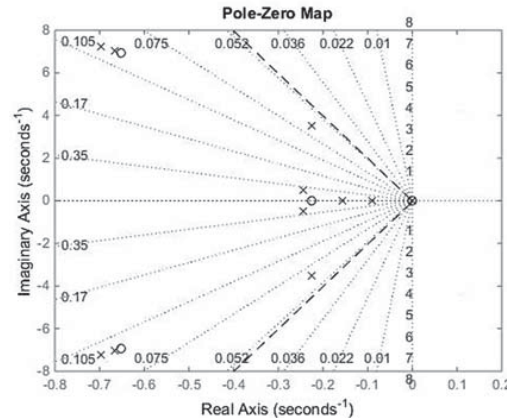


Fig. 7 Diagram of poles and zeros base case

C. Damping  $\xi \geq 8\%$

Fig. 8 shows the Pole-Zero map for an increasing the damping ratio higher than 8%. Table IV presents the gains of both controllers with a damping ratio higher than 8%.

	K	$T_w$	$T_1$	$T_2$	$\xi$
PSS	53.336	10.0s	0.06s	0.02s	0.08
POD	52.911	10.0s	0.06s	0.02s	

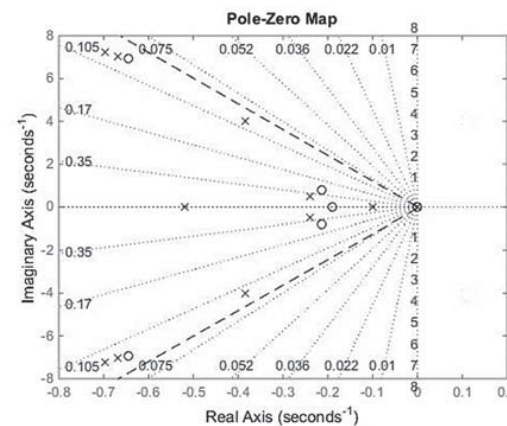


Fig. 8 Diagram of poles and zeros with  $\xi \geq 8\%$

D. Damping  $\xi \geq 10\%$

Fig. 9 shows the Pole-Zero map for an increasing the damping ratio higher than 10%. Table V presents the gains of both controllers with a damping ratio higher than 10%.

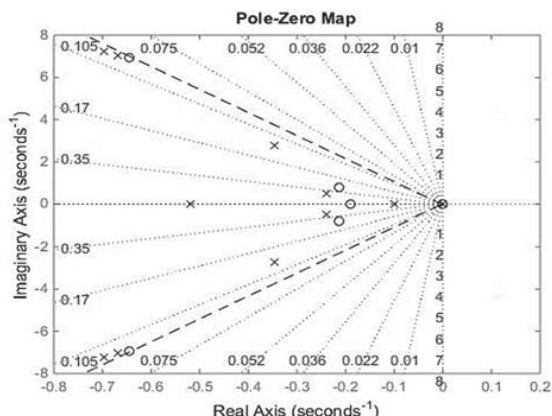


Fig. 9 Diagram of poles and zeros with  $\xi \geq 10\%$

TABLE V  
OPTIMIZED CONTROLLER PARAMETERS – DAMPING 10%

	K	$T_w$	$T_1$	$T_2$	$\xi$
PSS	71.570	10.0s	0.06s	0.02s	0.10
POD	67.881	10.0s	0.06s	0.02s	

Figs. 7-9 show the dominant eigenvalues of the test system with PSS and POD controllers, and it is clear that the system with both controllers is stable.

IV. COMPARISON WITH A DIFFERENT OBJECTIVE FUNCTION

The proposed method is compared with [21]. For a damping of 5%, the gains obtained with the optimization problem formulated (CDI) at [21] are  $K_{PSS} = 69.9$  and  $K_{POD} = 64.7$ .

Figs. 10-13 show the comparison results. It can see that the controllers computed by the proposed method preserve the stability under large disturbances. When the fault occurs, the controllers damp the electromechanical oscillations presented in the system.

It is also clear that when the gain of both controllers is increased, the local modes shift more to the left semi plane, and the damping ratios are more favorable.

Fig. 11 shows the electrical power oscillations at generator 2 for the different objective function. As it is observed in the first period the oscillation, the power electric decreases when the fault occurs, but the responses of both controllers are fast, and after few seconds, the electrical power returns to the original value time.

Fig. 12 shows the oscillations in the frequency at generator 2. Once the fault occurs, the machine accelerates. The frequency oscillations are different for both techniques although, with the proposed method, generator 2 has decelerations softer than CDI. The frequency at generator 2 stabilizes faster than other generators because the local controller located in this machine.

Fig. 13 shows the SVC voltage bus for the different objective functions. The peak value of voltage (1.07) which has an overshoot (7.1%) is normalized in the second swing, entering the safe operating limit. The POD controller provides damping overall to the power system and improves the transient stability.

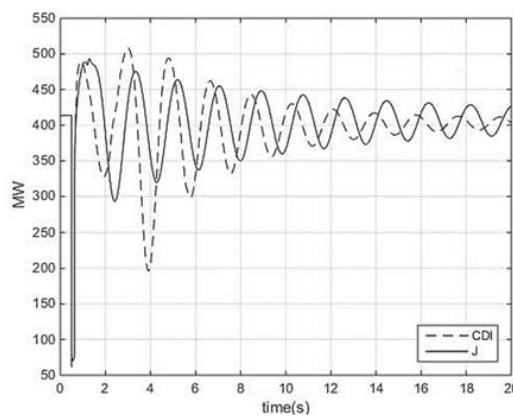


Fig. 10 Active power flow through interconnection of area 1 to area 2- with supplementary control

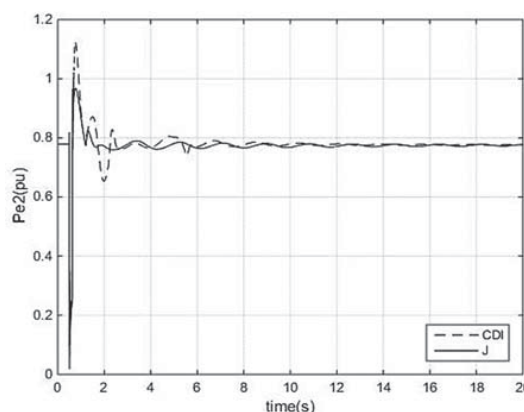


Fig. 11 Power Generation at Generator 2

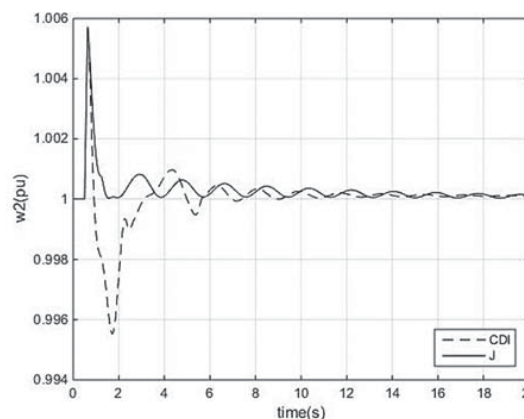


Fig. 12 Frequency behavior - Generators 1 and 2

V. CONCLUSION

This paper has presented a methodology for the coordinated tuning of the PSS and POD controller based on an algorithm optimization. The methodology is based on the linearized power system model and parameter-constrained nonlinear optimization technique.

The reduced model can be used to facilitate the design of damping controllers and it has been demonstrated with a

reduced model of approximately  $1/5^{th}$  of the size of the original model.

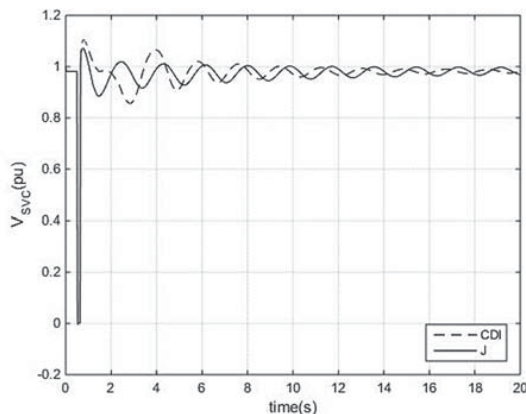


Fig. 13 SVC bus voltage behavior

The results obtained from the test system using the coordinated tuning method revealed that the adequate damping could be achieved by increasing the gains of both controllers.

Although the SVC is simulated in the proposed test system, the algorithm is generally applicable to the other types of FACTS device.

#### ACKNOWLEDGMENT

This work was financed with resources from COLCIENCIAS-UNIANDÉS under the program "Jovenes Investigadores 2014, convocatoria 645 de 2014".

#### REFERENCES

- [1] P. Kundur, *Power System Stability and Control*, McGraw-Hill, 1994, ch. 2 and 12.
- [2] G. Rogers, *Power system Oscillations*, The Kluwer International Series in Engineering and Computer Science. Kluwer Academic Pub, 1999, ch. 1, 2, and 7.
- [3] L.J Cai and I. Erlich, "Fuzzy coordination of FACTS controllers for damping power system oscillations," *In Modern Electric Power Systems Proc of the International Symposium Wroclaw*, September 11-13, 2002, pp 251-256.
- [4] K. C. Rout and P. C. Panda, "Performance analysis of power system dynamic stability using Fuzzy logic based PSS for positive and negative value of K5 constant," *Computer, Communication and Electrical Technology (ICCCET)*, 2011 International Conference on, Tamilnadu, 2011, pp. 430-435.
- [5] X. Lei, E. N. Lerch and D. povh, "Optimization and coordination of damping controls for improving systems dynamic performance," *IEEE Trans. Power Systems*, Vol. 16, August 2001, pp 473-480.
- [6] J. J. Sanchez Gasca and J. H. Chow, "Power system reduction to simplify the design of damping controllers for inter-area oscillations," *IEEE Trans. Power Systems*, Vol. 11, No 3, August 1996, pp 1342-1349.
- [7] P. Pourbeik and M. J. Gibbard, "Simultaneous coordination of power system stabilizers and FACTS device stabilizers in a multimachine power system for enhancing dynamic performance," *IEEE Trans Power Systems*, Vol 13, No 2, 1998, pp 476-479.
- [8] D. Arnatovic and J. Medanic, "Design of decentralized multi-variable excitation controller in multi-machine power systems by projective controls," *IEEE Trans Energy Conversion*, Vol EC-2, no 4, December 1987, pp 598-604.
- [9] M. G. Safonov, R. Y. Chiang, "A Schur Method for Balanced-Truncation Model reduction," *IEEE Transactions on Automatic Control*, Vol. 34, No 7, July 1989, pp 729-733.
- [10] B. Moore, "Principal Component Analysis in Linear Systems: Controllability, Observability, and Model Reduction," *IEEE Transactions on Automatic Control*, Vol. AC-26, No 1, February 1981, pp 17-31.
- [11] Alan J. Laub, Michael T. Heath, Chris C. Paige, Robert C. Ward, "Computation of System Balancing Transformations and their Applications of Simultaneous Diagonalization Algorithms," *IEEE Transactions on Automatic control*, Vol AC-32, No 2, February 1987, pp 115-122.
- [12] B. Pal, B. Chaudhuri, *Robust Control in Power Systems*, Springer, 2005, ch. 3 and ch. 5.
- [13] E. V. Larsen and D. A. Swann, "Applying Power System Stabilizers Part II: Performance Objectives and Tuning Concepts," in *IEEE Transactions on Power Apparatus and Systems*, vol. PAS-100, no. 6, June 1981, pp. 3025-3033.
- [14] K. R. Padiyar, *Power System Dynamics Stability and Control*. Jhon Wiley, Singapore, 1996, pp. 257-291.
- [15] R. Narne, P. C. Panda, J. P. Therattil, "Genetic algorithm based simultaneous coordination of PSS and FACTS controllers for power oscillations damping," *Sustainable Energy Technologies (ICSET), 2012 IEEE Third International Conference on*, Kathmandu, 2012, pp. 85-90.
- [16] M. A. Abido, "Design of PSS and STATCOM-based damping stabilizers using genetic algorithms," *2006 IEEE Power Engineering Society General Meeting*, Montreal, Que., 2006, pp. 1-8.
- [17] M. Hajizadeh and J. Sadeh, "Simultaneous coordination and tuning of PSS and FACTS for improving damping by genetic algorithm," *Electric Utility Deregulation and Restructuring and Power Technologies (DRPT), 2011 4th International Conference on*, Weihai, Shandong, 2011, pp. 1311-1315.
- [18] Klein, Rogers, Moorthy and Kundur: "Analytical investigation of factors influencing PSS performance," *IEEE Trans. on EC*, Vol. 7, No 3, September 1992, pp 382-390.
- [19] M. Eslami, H. Shareef, A. Mohamed, "Coordinated design of PSS and TCSC controller for power system stability improvement," *IPEC 2010 Conference Proceeding*, October 2010, pp 433-438.
- [20] N Islam, H. Shareef, A. Mohamed "Power system stabilizer design using BAT optimization algorithm in multimachine power system," *2013 IEEE Student Conference on Research and Development*, pp 540-544, December 2013.
- [21] Cai L.J, I. Erlich, "Simultaneous coordinated tuning of PSS and FACTS damping controllers in large power systems," *IEEE Transactions on Power Systems*, Vol 20, pp 294 - 300, February 2005.



**José D. Herrera** was born in Cartagena, Colombia, in 1986. He received his B.Sc degrees in Electrical Engineer from Universidad Tecnológica de Bolívar in 2010, Cartagena, Colombia. He worked in the Department of Electrical Engineering and Electronics at Universidad de los Andes, as a graduate assistant. He is now an M. Sc candidate at Universidad de los Andes, Bogotá, Colombia. He is interested in the application of robust control in power systems. (e-mail: hm.jose10@uniandes.edu.co).



**Mario A. Ríos** received a degree in electrical engineering in 1991 and an M.Sc. Degree in electrical engineering in 1992, both from Universidad de los Andes, Bogotá, Colombia. He received a Ph.D. degree in electrical engineering from INPG-LEG, France, in 1998, and a Doctoral degree in engineering from Universidad de los Andes, in 1998. He worked as a consultant engineer in ConCol, Bogotá, Colombia, during 12 years. Also, he was a Research Associate at the University of Manchester (formerly, UMIST). Currently, he is Full Professor at the Department of Electrical Engineering, School of Engineering, Universidad de Los Andes, Bogotá, and director of the Power and Energy Group of this university (e-mail: mrios@uniandes.edu.co).